

High-performance InAlGaN/GaN enhancement-mode MOS-HEMTs grown by pulsed metal organic chemical vapor deposition

Ya-Chao Zhang(张雅超), Zhi-Zhe Wang(王之哲), Rui Guo(郭蕊), Ge Liu(刘鸽), Wei-Min Bao(包为民), Jin-Cheng Zhang(张进成), Yue Hao(郝跃)

Citation: Chin. Phys. B . 2019, 28(1): 017301. **doi:** 10.1088/1674-1056/28/1/017301
Journal homepage: http://cpb.iphy.ac.cn; http://iopscience.iop.org/cpb

What follows is a list of articles you may be interested in

Groove-type channel enhancement-mode AlGaN/GaN MIS HEMT with combined polar and nonpolar AlGaN/GaN heterostructures

Xiao-Ling Duan(段小玲), Jin-Cheng Zhang(张进成), Ming Xiao(肖明), Yi Zhao(赵一), Jing Ning(宁静), Yue Hao(郝跃)
Chin. Phys. B . 2016, 25(8): 087304. **doi:** 10.1088/1674-1056/25/8/087304

Fabrication and characterization of the normally-off N-channel lateral 4H-SiC metal-oxide-semiconductor field-effect transistors

Qing-Wen Song(宋庆文), Xiao-Yan Tang(汤晓燕), Yan-Jing He(何艳静), Guan-Nan Tang(唐冠男),Yue-Hu Wang(王悦湖), Yi-Meng Zhang(张艺蒙), Hui Guo(郭辉), Ren-Xu Jia(贾仁需),Hong-Liang Lv(吕红亮), Yi-Men Zhang(张义门), Yu-Ming Zhang(张玉明)
Chin. Phys. B . 2016, 25(3): 037306. **doi:** 10.1088/1674-1056/25/3/037306

Investigation of trap states in Al_2O_3 InAlN/GaN metal-oxide-semiconductor high-electron-mobility transistors

Zhang Peng, Zhao Sheng-Lei, Xue Jun-Shuai, Zhu Jie-Jie, Ma Xiao-Hua, Zhang Jin-Cheng, Hao Yue
Chin. Phys. B . 2015, 24(12): 127306. **doi:** 10.1088/1674-1056/24/12/127306

Recovery of PMOSFET NBTI under different conditions

Cao Yan-Rong, Yang Yi, Cao Cheng, He Wen-Long, Zheng Xue-Feng, Ma Xiao-Hua, Hao Yue
Chin. Phys. B . 2015, 24(9): 097304. **doi:** 10.1088/1674-1056/24/9/097304

Non-recessed-gate quasi-E-mode double heterojunction AlGaN/GaN high electron mobility transistor with high breakdown voltage

Mi Min-Han, Zhang Kai, Chen Xing, Zhao Sheng-Lei, Wang Chong, Zhang Jin-Cheng, Ma Xiao-Hua, Hao Yue
Chin. Phys. B . 2014, 23(7): 077304. **doi:** 10.1088/1674-1056/23/7/077304

RAPID COMMUNICATION

Pressure-mediated contact quality improvement between monolayer MoS_2 and graphite*

Mengzhou Liao(廖梦舟)[1,2], Luojun Du(杜罗军)[1,2,6], Tingting Zhang(张婷婷)[1,2,3], Lin Gu(谷林)[1,2], Yugui Yao(姚裕贵)[3], Rong Yang(杨蓉)[1,2,4], Dongxia Shi(时东霞)[1,2,4,†], and Guangyu Zhang(张广宇)[1,2,4,5,‡]

[1] *CAS Key Laboratory of Nanoscale Physics and Devices, Institute of Physics, Chinese Academy of Sciences, Beijing* 100190, *China*
[2] *School of Physical Sciences, University of Chinese Academy of Sciences, Beijing* 100190, *China*
[3] *Beijing Key Laboratory of Nanophotonics and Ultrafine Optoelecentronic Systems, School of Physics, Beijing Institute of Technology, Beijing* 100081, *China*
[4] *Beijing Key Laboratory for Nanomaterials and Nanodevices, Beijing* 100190, *China*
[5] *Collaborative Innovation Center of Quantum Matter, Beijing* 100190, *China*
[6] *Department of Electronics and Nanoengineering, Aalto University, Tietotie* 3, FI-02150, *Finland*

(Received 18 October 2018; revised manuscript received 11 November 2018; published online 30 December 2018)

Two-dimensional (2D) materials and their heterostructures have attracted a lot of attention due to their unique electronic and optical properties. MoS_2 as the most typical 2D semiconductors has great application potential in thin film transistors, photodetector, hydrogen evolution reaction, memory device, etc. However, the performance of MoS_2 devices is limited by the contact resistance and the improvement of its contact quality is important. In this work, we report the experimental investigation of pressure-enhanced contact quality between monolayer MoS_2 and graphite by conductive atom force microscope (C-AFM). It was found that at high pressure, the contact quality between graphite and MoS_2 is significantly improved. This pressure-mediated contact quality improvement between MoS_2 and graphite comes from the enhanced charge transfer between MoS_2 and graphite when MoS_2 is stretched. Our results provide a new way to enhance the contact quality between MoS_2 and graphite for further applications.

Keywords: MoS_2/graphite heterojunction, C-AFM, pressure, contact quality

PACS: 73.43.Fj, 73.50.–h, 68.65.–k **DOI:** 10.1088/1674-1056/28/1/017301

1. Introduction

Two-dimensional materials, such as transition metal dichalcogenides (TMDCs), have many exotic mechanical, electrical, and optical properties.[1] As one of the most widely studied TMDCs, molybdenum disulfide (MoS_2) has extremely good potential to be applied in fields such as thin film transistor (TFT),[2,3] photodetector,[4,5] light emitting device,[6] hydrogen evolution reaction,[7] memory device,[8] and gas sensor.[9] Although former works show that MoS_2 has high mobility,[2] the performance of its devices is greatly affected by the contact qualities with the electrodes. By using different kinds of metal electrodes,[10–13] phase engineering,[14] or graphene electrodes,[15,16] contact resistance of MoS_2 devices can be significantly reduced. However, it is still hard to form ohmic contact between metal and MoS_2 due to Fermi level pinning, where a finite Schottky barrier dominates the carrier transport.[17] Graphene is an optimized candidate to form good contact with MoS_2 and MoS_2/graphene heterojunction also has great potential in various devices applications.[7,16,18,19] It was reported that strain, including both tensile strain and compressive stain, offers a facile way to modulate the band structure of TMDCs.[20–23] However, the question of whether the strain will affect the contact between MoS_2 and graphene is barely unraveled.

In this work, we report the experimental investigation of pressure-enhanced contact quality between monolayer MoS_2 and graphite by conductive atom force microscope (C-AFM). We applied pressure on the MoS_2/graphite heterojunction by C-AFM tip and measured the current–voltage (I–V) relation simultaneously. We found that the I–V curve approaches linear shape as the pressure increases, which reveals the improving of contact quality between MoS_2 and graphite. It was clarified that this contact quality enhancing comes from the charge transfer between MoS_2 and graphite when MoS_2 is stretched. Our results provide a new way to improve contact quality between MoS_2 and graphite for further applications.

2. Experimental procedure

MoS_2 was epitaxial grown on mechanical exfoliated graphite on Si substrate with 300 nm SiO_2, described in our

*Project supported by the National Key R&D Program, China (Grant No. 2016YFA0300904), the Key Research Program of Frontier Sciences of the Chinese Academy of Sciences (Grant No. QYZDB-SSW-SLH004), the Strategic Priority Research Program (B) of the Chinese Academy of Sciences (Grant Nos. XDPB06 and XDB07010100), and the National Natural Science Foundation of China (Grant Nos. 61734001 and 51572289).

†Corresponding author. E-mail: dxshi@iphy.ac.cn
‡Corresponding author. E-mail: gyzhang@iphy.ac.cn

© 2019 Chinese Physical Society and IOP Publishing Ltd

previous work[24] (also see Methods for more details). As shown in Fig. 1(a) of the optical image, as-grown MoS_2 triangle domains on graphite have obviously preferred orientations and similar sizes. Figure 1(b) shows the atomic force microscope (AFM) image of an area zoomed in Fig. 1(a), and surfaces of both MoS_2 and graphite substrate are clean and free of contaminations. The height of as-grown MoS_2 triangle domains is ~ 0.85 nm, which is consistent with the height of monolayer MoS_2.[2] Selected area electron diffraction (SAED) pattern of transmission electron microscopy (TEM) in Fig. 1(c) was used to characterize the lattice alignment of MoS_2/graphite samples. The hexagonal diffraction spots of both MoS_2 and graphite have the same orientations, suggesting an either 0° or 60° twisting angle between the as-grown MoS_2 and graphite. Raman spectrum in Fig. 1(d) shows that E_{2g} peak is at 385.1 cm^{-1} and A_{1g} peak is at 406.5 cm^{-1}. The difference between E_{2g} and A_{1g} is 21.4 cm^{-1}, consistent with that of monolayer MoS_2. The photoluminescence spectrum in Fig. 1(e) shows that the MoS_2 layer has a strong and well sharp A exciton peak at 660 nm, indicating that the monolayer MoS_2 domains are of high quality. The G peak 581 nm and 2D peak 622 nm of graphene are marked in the spectrum.

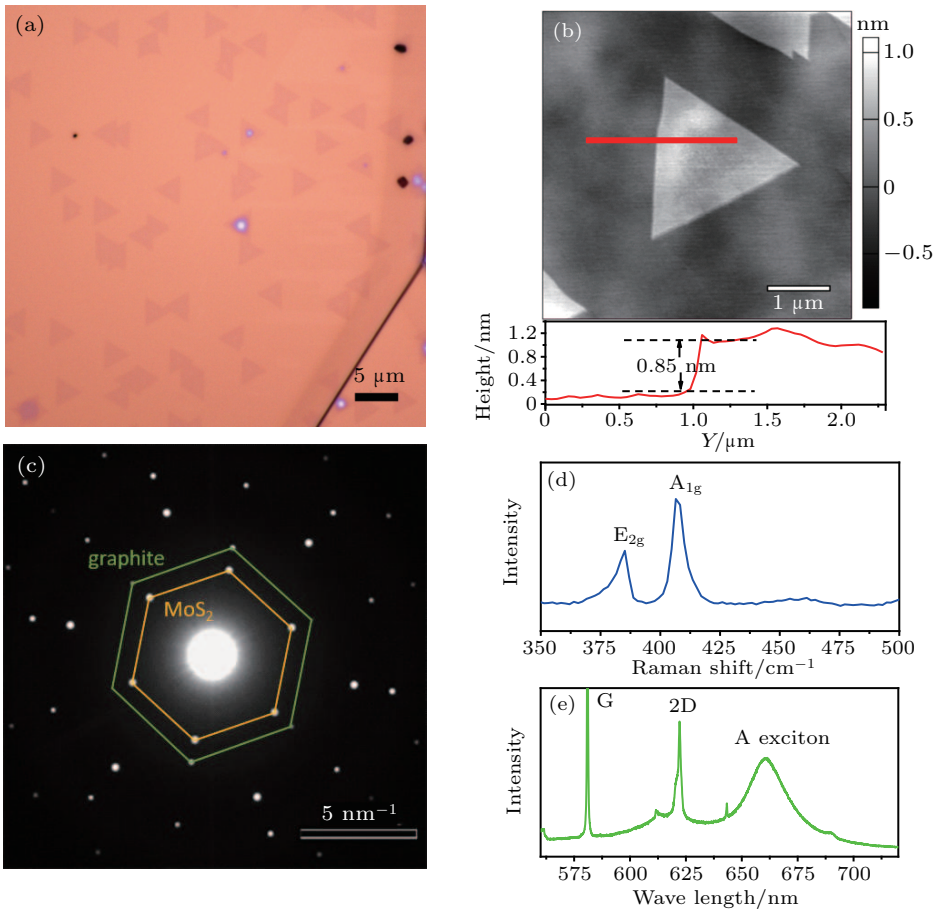


Fig. 1. Characterizations of MoS_2/graphite heterojunctions. (a) Optical image of as-grown MoS_2 triangle domains on graphite. (b) AFM image of a MoS_2 domain. (c) SAED pattern, (d) Raman spectrum, and (e) photoluminescence spectrum of the MoS_2/graphite heterojunction.

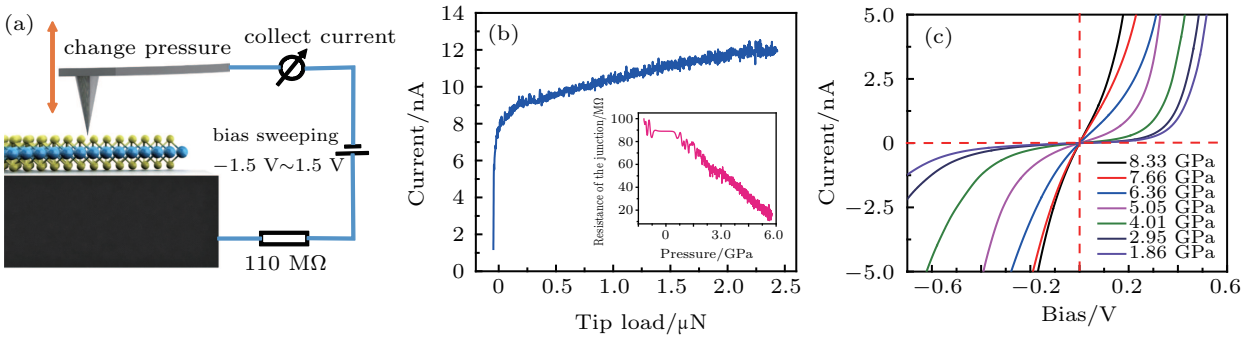


Fig. 2. The electrical behavior of MoS_2/graphite heterojunction under pressure. (a) Schematic of the measuring process and the circuit. (b) Tip–sample current as a function of tip load under bias of 1.5 V. The insert is the resistance of the MoS_2/graphite junction as a function of pressure. (c) *I*–*V* curves under different pressure.

We used C-AFM to test the electrical behavior of the MoS_2/graphite heterojunction under different pressure, and the setup is shown in Fig. 2(a). In the experiment, a metal coating tip was directly contact to the heterojunctions under controlled load. We swept sample-to-tip bias from −1.5 V to +1.5 V and collected the *I*–*V* curve of each load. To ensure the good contact between tip and heterojunction, the *I*–*V* curves were captured during the decompressing process. Figure 2(b) is the current under bias of 1.5 V as a function of tip load. It shows that the fluctuation of the current is low, suggesting the stable contact between tip and sample. For detail about C-AFM measurement please see Methods.

3. Experimental results and discussion

The center pressure of tip–sample contact was estimated by a standard Hertz module,[25] and the error of the estimate tip pressure is around 30% (see Methods). As illustrated in the insert of Fig. 2(b), under bias of 1.5 V, the resistance of the MoS_2/graphite junction monotonically decreases as increasing the pressure. This can be interpreted as the effect of both the reducing resistance of mental tip/MoS_2/graphite junction and the enlarging contact area caused by pressure. Figure 2(c) shows *I*–*V* curves under different pressure from 1.86 GPa to 8.33 GPa. Obviously, with increasing the pressure, *I*–*V* curve of the MoS_2/graphite heterojunction is approaching linear shape. This indicates that the contact quality is significantly improved under high pressure.

To further demonstrate the enhancing of contact quality between monolayer MoS_2 and graphite, we calculated the Schottky barrier at different pressure. From the thermal electron emission theory, the current is[26]

$$I = I_{\mathrm{sT}}(\mathrm{e}^{\frac{qV_{\mathrm{b}}}{nk_{\mathrm{B}}T}} - 1),$$

where I_{sT} is the dark saturation current, n is the ideality factor, T is the temperature, k_{B} is Boltzmann constant, and q is the electron charge. For large bias V_{b}, the −1 term is negligible. So

$$I = I_{\mathrm{sT}}\mathrm{e}^{\frac{qV_{\mathrm{b}}}{nk_{\mathrm{B}}T}}.$$

Taking ln in both sides,

$$\ln(I) = \ln(I_{\mathrm{sT}}) + \frac{q}{nk_{\mathrm{B}}T}V_{\mathrm{b}}, \tag{1}$$

I_{sT} can be written as

$$I_{\mathrm{sT}} = S \cdot A \cdot T^2 \mathrm{e}^{\frac{qV_0}{k_{\mathrm{B}}T}},$$

where V_0 is the Schottky barrier height, S is the contact area, and A is the Richardson's coefficient, which is 80.3 ± 18.4 A/cm^2/K.[27] Here, we use the Hertz model to estimate the contact area. For the case where the tip contacts a flat surface, the contact area can be written as

$$S = \pi a^2,$$

where[25]

$$a^3 = \frac{3}{4}R_{\mathrm{tip}}\left(\frac{1-\mu_{\mathrm{si}}^2}{E_{\mathrm{si}}} + \frac{1-\mu_{\mathrm{hetero}}^2}{E_{\mathrm{hetero}}}\right)F.$$

Here a is the contact radius, F is the tip load, and R_{tip} is the tip radius. we take $R_{\mathrm{tip}} = 28$ nm based on the commercial description of ASYLELEC-01 tip. E_{si}, E_{hetero}, and μ_{si}, μ_{hetero} are the elastic modulus and Poisson's ratio of silicon and heterojunction, which are 170 GPa, 36.5 GPa and 0.17, 0.25, respectively. Here we use the modulus of graphite to stand for the heterojunction.

Figures 3(a) and 3(b) are the plots of $\ln(I)$ as a function of positive and negative bias voltage at different pressure, respectively. Solid lines are experimental data and dots lines are fittings by using Eq. (1). The fittings are quite good at the high bias region. Figure 3(c) is the calculated Schottky barrier height as a function of pressure, which can be linearly fitted except few points around high and low pressure regions. It is clear that Schottky barrier height of both positive and negative bias region decreases when increasing pressure which contributes the improving of contact quality. It is also noted that Schottky barrier height of positive bias region is slightly bigger than that of negative bias region in Fig. 3(c). The asymmetry of Schottky barrier height is due to the difference of work function of graphite and Ir.

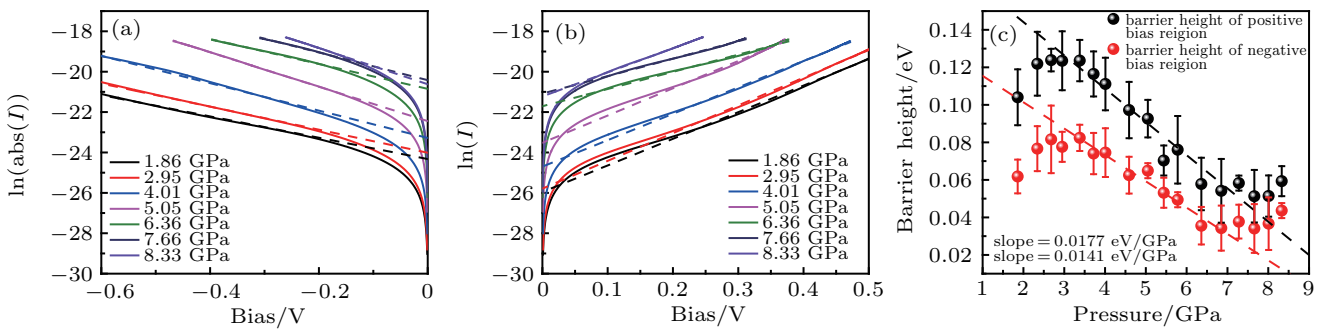


Fig. 3. The calculation of Schottky barrier height under different pressure. The natural logarithm of the current as a function of bias at (a) positive and (b) negative sample bias regions. The dashed lines represent fittings by using thermal electron emission theory. (c) Schottky barrier height as function of pressure. Dash lines are linear fittings.

We tried to reveal the intrinsic mechanism of this pressure-enhanced contact quality between monolayer MoS_2 and graphite. As shown in Figs. 4(a) and 4(b), in the control experiment of monolayer MoS_2 transferred on ITO substrate, the Schottky barrier height does not show a clear variation trend with the increase of pressure. This indicates that this pressure-enhanced contact quality is unique in MoS_2/graphite heterojunction. In our experiment, AFM tip not only applies pressure on MoS_2/graphite junction, but also deforms the contact area and stretches the MoS_2. According to the previous simulations, when the MoS_2 layer in the MoS_2/graphite heterojunction is stretched $\sim 2.7\%$, the bottom of the conduction band of MoS_2 will be below the Fermi level, while the Dirac point of graphene will be above the Fermi level. This results in the electrons transfer from graphene to MoS_2 and adds new electrons occupied states in MoS_2 conduction band.[28] As shown in Figs. 4(d) and 4(e), with this new electron occupied states in MoS_2 conduction band, electron can two-step tunnel through the barrier, which will significantly reduce the effective Schottky barrier. Consequently, in our experiments, this pressure-mediated contact quality improvement of graphite/MoS_2 heterojunction origins from the enhancing of charge transfer between MoS_2 and graphite when MoS_2 layer is stretched by AFM tip. It should be pointed out that the pressure in our experiment also reduces the interlayer distance between MoS_2 and graphite which will enhance the interlayer coupling. Besides, there is pristine tensile strain in MoS_2 layer due to 28% lattice mismatch between MoS_2 and graphite.[24]

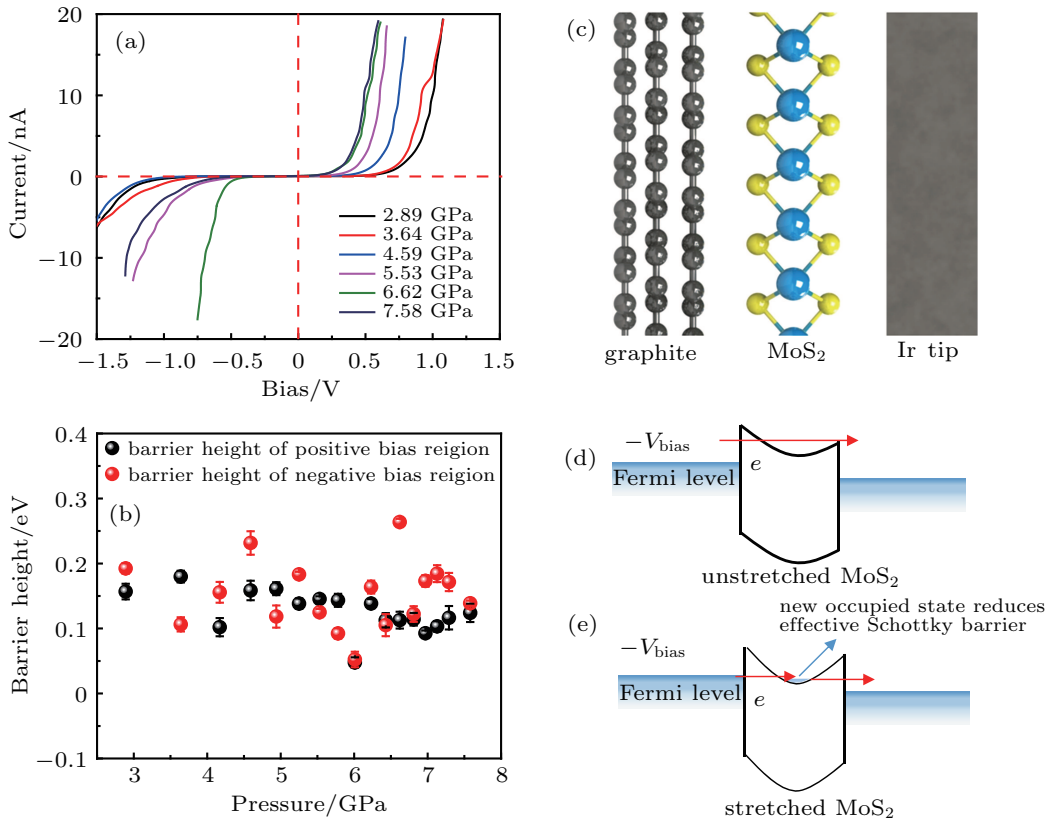


Fig. 4. Explanation of pressure-enhanced contact quality between MoS_2 and graphite under pressure. (a) *I*–*V* curves of metal tip/transferred MoS_2/ITO junction under different pressure. (b) Schottky barrier height of metal tip/transferred MoS_2/ITO junction as function of pressure. (c) Schematic illustration of metal tip–MoS_2–graphite contact. The band structure at negative sample bias of (d) upstretched MoS_2 and (e) stretched $\sim 2.7\%$ MoS_2.

4. Conclusion

We demonstrated pressure-enhanced contact quality between monolayer MoS_2 and graphite induced by pressure. This enhancement of the contact quality is due to the charge transfer between MoS_2 and graphite when MoS_2 is stretched. Our work provides a guidance in contacts engineering of MoS_2/graphite heterojunction by pressure, and may help to reduce the contact resistance in MoS_2 devices as well as other TMDCs devices contacted by graphene.

Appendix A: methods

Sample preparation The MoS_2 growth was performed in a three-temperature-zone chemical vapor deposition (CVD) chamber. S (Alfa Aesar, 99.9%, 4 g) and MoO_3 (Alfa Aesar, 99.999%, 50 mg) powders used as sources were loaded in two separate inner tubes and placed at zone-I and zone-II, respectively. Our substrates were loaded in zone-III. During the growth, with Ar/O_2 (gas flow rate: 75/3 sccm) as carrying gases, temperatures for the S-source, MoO_3-source, and wafer substrate were set at 115 °C, 530 °C, and 930 °C, respectively.

Thin graphite flakes were mechanically exfoliated from both HOPG and Graphenium graphite (Manchester Nanomaterials) and transferred on SiO_2 substrates for MoS_2 growth.

Sample characterizations PL and Raman characterizations were performed in a Horiba Jobin Yvon LabRAM HR-Evolution Raman system using a 532 nm laser excitation wavelength. SAED was performed in a TEM (Philips CM200) operating at 200 kV.

AFM and C-AFM scanning AFM imaging was performed by Asylum Research Cypher S with AC160 TS tip. C-AFM experiments were carried under ambient condition using ASYELEC-01, Ti/Ir coated Si tip, and the bias was applied on sample. We used the holder 901.730, current range ±20 nA, and noise 1.5 pA. We used a standard Sader's method[29] to calibrate the cantilever and the bending modulus of the ASYELEC-01 cantilever we used in the experiment is 2.56 nN/nm. The tip radius of ASYELEC-01 tip is 28 nm±40%. According to pressure $P_0 = 3F/(2\pi a^2)$, contact radius $a^3 = 3/4 \cdot R_{\text{tip}}((1-\mu_{\text{si}}^2)/E_{\text{si}} + (1-\mu_{\text{hetero}}^2)/E_{\text{hetero}})F_{\text{load}}$, so the error of estimate pressure is around 30%.

Acknowledgements

Guangyu Zhang and Dongxia Shi designed and supervised the research. Mengzhou Liao performed the AFM measurements and data analysis. Luojun Du performed the growth, TEM, and spectroscopic characterizations. Lin Gu performed TEM. Yugui Yao, Rong Yang, Dongxia Shi, and Guangyu Zhang helped analyze data. Mengzhou Liao, Dongxia Shi, and Guangyu Zhang wrote and all of the authors commented on the manuscript. The data and materials are available from the corresponding authors upon request.

References

[1] Wang Q H, Kalantar-Zadeh K, Kis A, Coleman J N and Strano M S 2012 *Nat. Nanotechnol.* **7** 699
[2] Radisavljevic B, Radenovic A, Brivio J, Giacometti V and Kis A 2011 *Nat. Nanotechnol.* **6** 147
[3] Wang H, Yu L, Lee Y H, Shi Y, Hsu A, Chin M L, Li L J, Dubey M, Kong J and Palacios T 2012 *Nano Lett.* **12** 4674
[4] Lopez-Sanchez O, Lembke D, Kayci M, Radenovic A and Kis A 2013 *Nat. Nanotechnol.* **8** 497
[5] Yin Z, Li H, Li H, Jiang L, Shi Y, Sun Y, Lu G, Zhang Q, Chen X and Zhang H 2012 *ACS Nano* **6** 74
[6] Sundaram R S, Engel M, Lombardo A, Krupke R, Ferrari A C, Avouris P and Steiner M 2013 *Nano Lett.* **13** 1416
[7] Li Y, Wang H, Xie L, Liang Y, Hong G and Dai H 2011 *J. Am. Chem. Soc.* **133** 7296
[8] Bertolazzi S, Krasnozhon D and Kis A 2013 *ACS Nano* **7** 3246
[9] Li H, Yin Z Y, He Q Y, Li H, Huang X, Lu G, Fam D W H, Tok A I Y, Zhang Q and Zhang H 2012 *Small* **8** 63
[10] Kaushik N, Nipane A, Basheer F, Dubey S, Grover S, Deshmukh M M and Lodha S 2014 *Appl. Phys. Lett.* **105** 113505
[11] Das S, Chen H Y, Penumatcha A V and Appenzeller J 2013 *Nano Lett.* **13** 100
[12] Chen J R, Odenthal P M, Swartz A G, Floyd G C, Wen H, Luo K Y and Kawakami R K 2013 *Nano Lett.* **13** 3106
[13] Kang J H, Liu W and Banerjee K 2014 *Appl. Phys. Lett.* **104** 093106
[14] Kappera R, Voiry D, Yalcin S E, Branch B, Gupta G, Mohite A D and Chhowalla M 2014 *Nat. Mater.* **13** 1128
[15] Liu Y, Wu H, Cheng H C, Yang S, Zhu E, He Q, Ding M, Li D, Guo J, Weiss N O, Huang Y and Duan X 2015 *Nano Lett.* **15** 3030
[16] Xie L, Liao M, Wang S, Yu H, Du L, Tang J, Zhao J, Zhang J, Chen P, Lu X, Wang G, Xie G, Yang R, Shi D and Zhang G 2017 *Adv. Mater.* **29** 1702522
[17] Allain A, Kang J H, Banerjee K and Kis A 2015 *Nat. Mater.* **14** 1195
[18] Roy K, Padmanabhan M, Goswami S, Sai T P, Ramalingam G, Raghavan S and Ghosh A 2013 *Nat. Nanotechnol.* **8** 826
[19] Yu L, Lee Y H, Ling X, Santos E J, Shin Y C, Lin Y, Dubey M, Kaxiras E, Kong J, Wang H and Palacios T 2014 *Nano Lett.* **14** 3055
[20] Conley H J, Wang B, Ziegler J I, Haglund R F, Pantelides S T and Bolotin K I 2013 *Nano Lett.* **13** 3626
[21] Manzeli S, Allain A, Ghadimi A and Kis A 2015 *Nano Lett.* **15** 5330
[22] Johari P and Shenoy V B 2012 *ACS Nano* **6** 5449
[23] Song S, Keum D H, Cho S, Perello D, Kim Y and Lee Y H 2016 *Nano Lett.* **16** 188
[24] Du L J, Yu H, Liao M Z, Wang S P, Xie L, Lu X B, Zhu J Q, Li N, Shen C, Chen P, Yang R, Shi D X and Zhang G Y 2017 *Appl. Phys. Lett.* **111** 263106
[25] Johnson K L 1985 *Contact Mechanics* (Cambridge: Cambridge University Press)
[26] Yu W J, Li Z, Zhou H L, Chen Y, Wang Y, Huang Y and Duan X F 2013 *Nat. Mater.* **12** 246
[27] Jahangir I, Uddin M A, Singh A K, Koley G and Chandrashekhar M V S 2017 *Appl. Phys. Lett.* **111** 142101
[28] Liu X and Li Z 2015 *J. Phys. Chem. Lett.* **6** 3269
[29] Sader J E, Chon J W M and Mulvaney P 1999 *Rev. Sci. Instrum.* **70** 3967